





## Article

# Experimental and Numerical Study of Biochar Fixed Bed Column for the Adsorption of Arsenic from Aqueous Solutions

Maria Rosaria Boni <sup>1,\*</sup>, Simone Marzeddu <sup>1,\*</sup>, Fabio Tatti <sup>2</sup>, Massimo Raboni <sup>3</sup>, Giuseppe Mancini <sup>4</sup>, Antonella Luciano <sup>5</sup> and Paolo Viotti <sup>1</sup>

- <sup>1</sup> Faculty of Civil and Industrial Engineering, Department of Civil, Constructional and Environmental Engineering (DICEA), Sapienza University of Rome, Via Eudossiana 18, 00184 Rome, Italy; mariarosaria.boni@uniroma1.it (M.R.B.); paolo.viotti@uniroma1.it (P.V.)
- <sup>2</sup> National Centre of Waste and Circular Economy, Italian Institute for Environmental Protection and Research (ISPRA), Via Vitaliano Brancati 48, 00144 Rome, Italy; fabio.tatti@isprambiente.it
- <sup>3</sup> Department Hydraulics and Environmental Engineering, Department of Civil Engineering and Architecture (DICAr), University of Pavia, Corso Strada Nuova 65, 27100 Pavia, Italy; massimo.raboni@gmail.com
- <sup>4</sup> Department of Electric Electronic and Computer Engineering (DIEEI), University of Catania, Viale Andrea Doria 6, 95125 Catania, Italy; giuseppe.mancini@unict.it
- <sup>5</sup> Resource Valorization Lab, Casaccia Research Centre, Department for Sustainability, Italian National Agency for New Technologies, Energy and Sustainable Economic Development (ENEA), Via Anguillarese 301, 00123 Rome, Italy; antonella.luciano@enea.it
- \* Correspondence: simone.marzeddu@uniroma1.it; Tel.: +39-06-44585514



**Citation:** Boni, M.R.; Marzeddu, S.; Tatti, F.; Raboni, M.; Mancini, G.; Luciano, A.; Viotti, P. Experimental and Numerical Study of Biochar Fixed Bed Column for the Adsorption of Arsenic from Aqueous Solutions. *Water* **2021**, *13*, 915. <https://doi.org/10.3390/w13070915>

Academic Editor: Laura Bulgariu

Received: 24 February 2021

Accepted: 24 March 2021

Published: 27 March 2021

**Publisher's Note:** MDPI stays neutral with regard to jurisdictional claims in published maps and institutional affiliations.



**Copyright:** © 2021 by the authors. Licensee MDPI, Basel, Switzerland. This article is an open access article distributed under the terms and conditions of the Creative Commons Attribution (CC BY) license (<https://creativecommons.org/licenses/by/4.0/>).

**Abstract:** Two laboratory tests were carried out to verify the suitability of an Italian commercial biochar as an adsorbing material. The chosen contaminant, considered dissolved in groundwater, was As. The circular economic concept demands the use of such waste material. Its use has been studied in recent years on several contaminants. The possibility of using an efficient material at low cost could help the use of low-impact technologies like permeable reactive barriers (PRBs). A numerical model was used to derive the kinetic constant for two of the most used isotherms. The results are aligned with others derived from the literature, but they also indicate that the use of a large amount of biochar does not improve the efficiency of the removal. The particular origin of the biochar, together with its grain size, causes a decrease in contact time required for the adsorption. Furthermore, it is possible that a strong local decrease in the hydraulic conductivity does not allow for a correct dispersion of the flow, thereby limiting its efficiency.

**Keywords:** arsenic; biochar; breakthrough curve analysis; continuous-flow systems; contaminated groundwater; numerical model

## 1. Introduction

Aquifers are the largest freshwater reservoir in the world, accounting for over 97% of all freshwater on Earth [1]. For many years, groundwater has been contaminated by an increasing number of chemicals produced by human activities such as agriculture, industrial procedures, and waste disposal [2]. Many solutes introduced into the hydrological environment are reported as contaminants, whose concentrations reach levels that are considered harmful [3].

Several aquifers (first and/or second aquifer) from which drinking water is drawn are contaminated by arsenic worldwide [4–9]. Arsenic is a metalloid which can be found into two different forms: amorphous yellow and crystalline gray/metallic [10].

Arsenic is a natural contaminant in the form of arsenates ( $\text{As}^{+5}$ ) and arsenites ( $\text{As}^{+3}$ ) [11]. Both forms are toxic, non-biodegradable, and can travel through the food chain [12]. Arsenite is more dangerous than arsenate, and can have serious carcinogenic effects. Long

periods of exposure can lead to tumors of the skin or of internal organs such as the liver, colon, or brain [13].

In order to prevent these effects, water is often treated to reduce the arsenic concentration to below the maximum admitted limit for drinking water, which has been set at below 10 µg/L by the World Health Organization (WHO) [14].

In the literature, different technologies for the removal of the As forms are reported [15–21]. The technologies are mainly based on oxidation/reduction [22], precipitation/dissolution [23], ion exchange [24], adsorption/desorption [25], and membrane filtration (e.g., nanofiltration) [19]. Adsorption is the most used technology [26–28]. It is based on the capacity of a surface (adsorbent) to retain molecules, atoms, or ions of substances in solid, liquid, or gaseous states (adsorbate) [29,30].

In many studies, different adsorbents have been investigated for arsenic removal from contaminated water, such as iron hydroxide [31], activated carbon [32], and active alumina [33]. In Table 1, their concentration ranges and theoretical adsorption capacities are shown.

**Table 1.** Adsorbent materials investigated for arsenic adsorption from contaminated water.

Adsorbent Media	As Concentration (µg/L)	pH (-)	Average Size (mm)	Specific Surface (m <sup>2</sup> /g)	Adsorption Capacity (mg/g)	References
Alumina APS	400–600	6.5–7.0				[34]
Alumina AMESO			0.106	155	8.310–9.223	
Alumina APS-TiO <sub>2</sub>			0.020	110	19.800	
250 °C			0.106	155	9.162–10.448	
Alumina APS-TiO <sub>2</sub>	20	7 ± 0.1	0.106	155	8.500	[35]
450 °C						
Granular ferric hydroxides			0.930	120–200	0.431	
			0.600	300	0.250	
	10,000	6.0	1.400	300	0.286	[36]
Magnetite nanoparticles						
			9 × 10 <sup>−6</sup>	n.r.	8.25	
PAC-CeO <sub>2</sub>	330	7.8	n.r.	1050	~12.000	[37]
GAC	100	6.0	300–600 × 10 <sup>−3</sup>	1124	0.180–0.130	[38]
GAC-Fe				876	0.300–0.440	

These adsorbents generally provide a high level of removal efficiency; however, they are expensive and often require regeneration phases or final disposal. In this study, biochar was utilized as an alternative adsorbent material to remove arsenic from contaminated water [39].

Biochar is a vegetable carbon obtained from the pyrolysis of different types of vegetable biomass or green waste [40]. It is a low-density, carbonized material produced by the combustion of biomass at low temperatures (between 450 °C and 550 °C) with minimal oxygen content [41]. Initially associated with the issue of waste management [42,43], interest in this material has grown enormously due to its ability to improve the physical, chemical, biological, and mechanical characteristics of soil [44,45].

Furthermore, its application to soils is practiced in order to achieve two other objectives: to increase soil fertility [46] and to contribute to the mitigation of climate change through the reduction of CO<sub>2</sub> and N<sub>2</sub>O emissions [47,48].

The production costs are negligible, the raw material is recovered at a minimal cost as waste material [49,50], and the pyrolysis is almost completely self-powered by the syngas produced by the same plant, ensuring minimum energy and economic consumption [51,52]. Thus, biochar may represent a sustainable material [53–55]. It can be used for various purposes, such as remediation of contaminated sites [56] or water treatment as a low-cost adsorbent [57].

This paper describes the results of an experimental and numerical study carried out to evaluate the suitability of using virgin coniferous wood biochar as an adsorbent medium. Two column tests were performed in continuous flow condition to investigate the capacity of commercial biochar to adsorb dissolved arsenic from contaminated groundwater.

An implemented, one-dimensional numerical model was also used to simulate the interaction between biochar and arsenic. The numerical model was conducted in order to investigate the influence of different operative parameters, such as the flow and the arsenic concentration in the contaminated water, on the effectiveness of the technology.

## 2. Materials and Methods

### 2.1. Materials Used for the Laboratory Tests

The laboratory tests were performed using a solution of arsenic and biochar mixed with different percentages of quartz sand. The used biochar consisted of virgin woody biomass (mainly pine wood) [58] derived from forest management activities (forestry) with a predefined grain size obtained by mechanical treatment (chipping).

The material complies with quality classes A1/A2 of UNI EN ISO 17225-4:2014 and the steps of the production process are described in a recently published paper [59]. The producer company carried out the chemical–physical characterization of the raw material in order to verify the necessary requirements for the request of the Italian certification as a soil improver, according to the Italian Law n. 75/2010.

The grain size of the sand was estimated by laboratory measurements [60,61] and the hydraulic conductivity was evaluated using the formula proposed by Hazen.

Table 2 reports the values of the measured chemical–physical parameters of the two materials and the analytical methods or reference laws used for the characterization.

**Table 2.** Main physical and chemical properties of the biochar and the quartz sand.

Material	Parameter	Unit	Value	Method
Biochar	Apparent bulk density compacted in the laboratory	kg/L	0.142	UNI EN 13040:2008
	pH	-	12.4 ± 0.46	UNI EN 13040:2008 + UNI EN 13037:2012
	Electric conductivity	mS/m	802 ± 13	UNI EN 13040:2008 + UNI EN 13038:2012
	Humidity	% m/m	5.3 ± 0.53	UNI EN 13040:2008
	Ash content (550 °C)	% m/m	31.26 ± 3.13	UNI EN 14775:2010
	Particle-size fraction < 5 mm	% m/m s.s.	100 ± 10	UNI EN 15428:2008
	Particle-size fraction < 2 mm	% m/m s.s.	97 ± 10	UNI EN 15428:2008
Quartz Sand	Particle-size fraction < 0.5 mm	% m/m	70 ± 7	UNI EN 15428:2008
	Dry density	kg/L	2.65	UNI EN 13242
	Medium grain size d <sub>50</sub>	µm	700	UNI EN 13242
	Medium grain size d <sub>10</sub>	µm	450	UNI EN 13242
	Medium grain size d <sub>60</sub>	µm	800	UNI EN 13242
	Hydraulic conductivity	m/s	3.0 × 10 <sup>−3</sup>	-

The arsenic solution used for the tests was obtained from a stock solution containing 3.125 g/L of As(V). It was prepared by dissolving sodium arsenate heptahydrate (Na<sub>2</sub>HAsO<sub>4</sub>·7H<sub>2</sub>O) [62], which has a solubility of 39 g/100 mL, into Milli-Q water at a temperature (T) of 21 ± 0.1 °C.

Proper dilution of the stock solution in fresh water allowed us to obtain the required arsenic concentration of 1 mg/L for the experimental tests. The arsenic solution was stored at T = 4 °C before use.

## 2.2. Experimental Apparatus and Test Procedure

The column tests were carried out using the experimental apparatus described in [63,64]. It was composed of a Pyrex glass column with an internal diameter of 8 cm and a length of 60 cm, a peristaltic pump, and a tank to stock the inflowing solution.

The column was filled with different elements, as shown in Figure 1a. The reactive zone, composed of a biochar and sand mixture, was in the middle of the column, while a filter zone was situated at either end of the column (one at the top and one at the bottom). The filter zones were composed of two layers: glass beads and quartz sand. The bottom filter was used to prevent the materials from escaping from the column outlet [65], and the upper filter to assure the best distribution of the inlet solution.

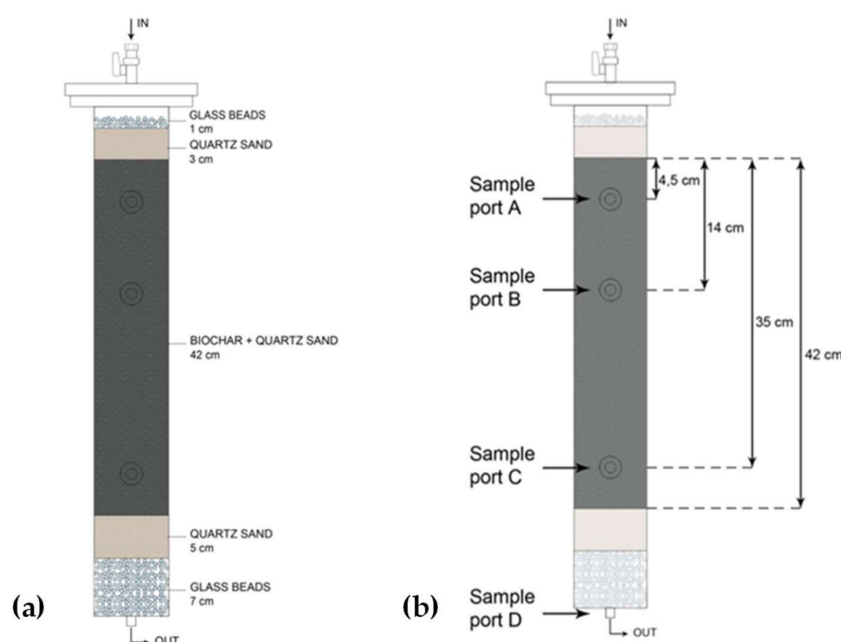


**Figure 1.** (a) Identification of the layer thicknesses of the elements within the column; (b) arrangement of the four column sample ports.

Two tests were carried out using different volume ratios of biochar and sand in the reactive zone. In Test 1, a biochar–sand volume ratio of 7:100 was used, while in Test 2, a ratio of 3:100 was used.

The column was equipped with sample ports positioned along the reactive zone and at the outlet in order to monitor the process inside the column (Figure 1b).

The column tests were performed following the procedure described by the authors of [66,67]. Firstly, the column was saturated with deionized water, then a solution containing 1 mg/L of As (at pH 7.5) was continuously fed into the top of the column through the peristaltic pump with a constant flow rate equal to 5 mL/min.

During the tests, water samples were collected from the ports in order to monitor the arsenic concentration along the column over time. The samples were filtered by 1  $\mu\text{m}$  and 0.45  $\mu\text{m}$  syringe filters (25 mm FLL/MLL Acrylic Yellow and white membranes, GVS Filter Technology, Morecambe, UK) [68] and analyzed for the residual As concentration in the solution. The total arsenic concentration in the aqueous phases was determined using mass spectrometry with an inductive plasma source (Perkin-Elmer® Model NexION 300x ICP-MS, Waltham, MA, USA), whose detection limit was 1  $\mu\text{g/L}$ .

The calibration curve was determined using Standard Methods 3125 [69] and total arsenic solutions at four concentrations (0, 10, 50, and 100  $\mu\text{g/L}$  As tot).

### 2.3. Numerical Model

A numerical model was conducted in a MATLAB environment to reproduce the laboratory tests. To simulate the solute transport through the saturated porous media, the model utilizes the classical advection–dispersion equation (1):

$$\frac{\partial C}{\partial t} + u_i \frac{\partial C}{\partial x_i} = \frac{\partial C}{\partial x_i} (D_{ij} \frac{\partial C}{\partial x_j}) \quad (1)$$

where  $C$  is the solute concentration ( $\text{M L}^{-3}$ ),  $t$  is the time ( $\text{T}$ ),  $x_i$  are the axes ( $\text{L}$ ),  $u_i$  are the components of velocity vector ( $\text{L T}^{-1}$ ), and  $D_{ij}$  is the hydrodynamic dispersion tensor ( $\text{L}^2 \text{T}^{-1}$ ).

Equation (1) can be considered as one-dimensional because the length of the column used for laboratory tests is much larger than its diameter, so the motion mainly occurs along the  $x$ -axis. Furthermore, for the characteristics of the prepared filling material, the sample can be considered homogeneous, so, porosity as well as hydrodynamic dispersion are constant along the whole column.

The motion in the column was assured from a pump connected to the exit of the column, in this way the seepage velocity ( $u$ ) was calculated from Equation (2):

$$u = \frac{Q}{A \times p} \quad (2)$$

where  $Q$  is the solution flow rate (equal to  $5 \text{ mL/min}$ ),  $A$  is the column section, and  $p$  is the porosity.

The value of the hydraulic dispersion coefficient (that coincides with mechanical dispersion) was calibrated, and the dispersivity value ( $D$ ) was determined for the two tests by means of (3):

$$D = \frac{\alpha_L u^2}{|u|} \quad (3)$$

The estimated value of  $\alpha_L$  is  $1.3 \times 10^{-2}$  for Test 1 and  $1.5 \times 10^{-2}$  for Test 2. The obtained values are in accordance with the values estimated using the relation proposed by Pickens and Grisak [70].

In order to consider the affinity of the solute for adsorption onto solid particles of biochar, the adsorption term is incorporated into the advection–dispersion Equation (1) [71] as follows:

$$\frac{\rho_b}{p} \frac{\partial S}{\partial t} + \frac{1}{p} \frac{\partial C}{\partial t} = \frac{D}{p} \frac{\partial^2 C}{\partial x^2} - \frac{u}{p} \frac{\partial C}{\partial x} \quad (4)$$

where  $S$  is the amount of solute absorbed on the biochar particles,  $p$  is the porosity, and  $\rho_b$  is the bulk density ( $\text{M L}^{-3}$ ). In order to investigate the most suitable isotherm [72] to describe the contaminant partition (adsorbed/dissolved), linear and Langmuir [73] isotherms were implemented in the numerical model. The two isotherms are respectively expressed as:

$$S = K_d C \quad (\text{Linear}) \quad (5)$$

$$S = \frac{q_{\max} K_L C}{1 + K_L C} \quad (\text{Langmuir}) \quad (6)$$

where  $C$  is the concentration of As in solution ( $\text{M L}^{-3}$ ) at equilibrium,  $q_{\max}$  is the maximum As uptake per unit of adsorbent ( $\text{M M}^{-1}$ ),  $K_L$  is the Langmuir equilibrium constant related to the free energy of adsorption ( $\text{L}^3 \text{M}^{-1}$ ), and  $K_d$  is the adsorbent coefficient ( $\text{L}^3 \text{M}^{-1}$ ).

Equation (4) is numerically solved using the explicit finite difference technique proposed by Karahan [74]. The technique is based on the Saulvey scheme [75] and it gives highly accurate results even for high values of the Courant number.

The one-dimensional simulation domain was divided into a regular grid with defined spacing ( $D_z$ ). As boundary conditions, the Dirichlet (top) and the Neumann (bottom) conditions were used.

### 3. Results and Discussion

Experimental data collected during the two column tests were compared to investigate the suitability of biochar to remove arsenic from water.

In this investigation, the influence of the biochar quantity on the removal process (Figure 2) was considered.

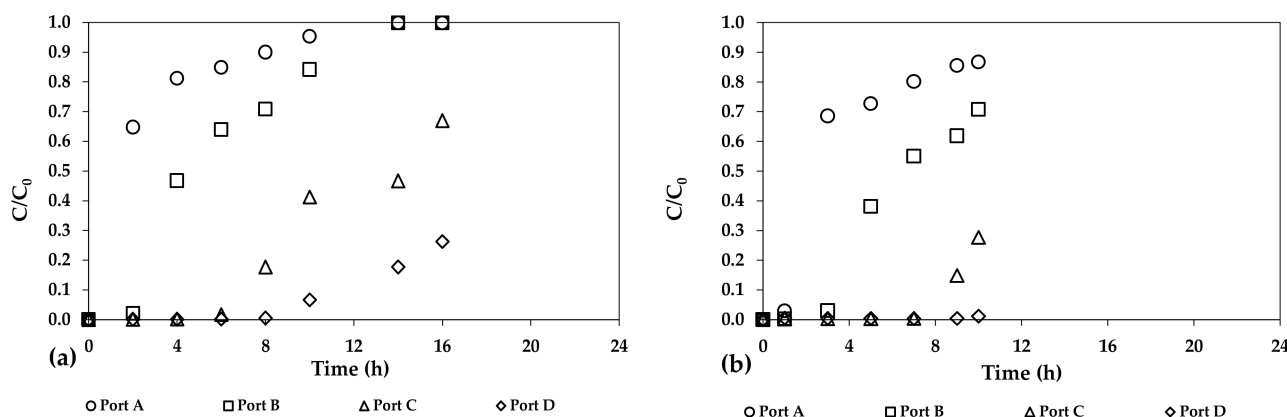


**Figure 2.** Breakthrough curves for Test 1 (a) and Test 2 (b) with respective biochar–sand volume ratios of 7:100 and 3:100.

The pH and the redox potential (ORP, mV) are the most important factors for controlling the speciation of arsenic [76].

In fact, within the samples collected during all the tests, the pH and the ORP were constant at  $7.5 \pm 0.2$  and  $800 \pm 100$  mV, respectively. Therefore, it is evident that arsenates ( $\text{HAsO}_4^{2-}$ ) remained dominant [77].

Concerning this point, to our surprise, the breakthrough curves of the tests show a higher adsorption of As in Test 2 (biochar–sand volume ratio of 3%) than in Test 1 (biochar–sand volume ratio of 7%).

This result is surely related to the extremely small biochar grain size leading to a smaller porosity, and therefore a lower availability, of the active sites of the material.

This effect causes the generation of zones with lower permeability, which probably reduces the overall surface of the biochar available to interact with the solute. In addition, the higher effective velocity in Test 1 (due to the lower porosity) reduces the contact time between the biochar and the dissolved arsenic.

The numerical model validates the results of the laboratory tests when comparing the breakthrough experimental curves with the numerical ones (Figures 3 and 4). Linear and Langmuir isotherms were implemented in the model in order to evaluate their ability to reproduce the experimental data.

A preliminary calibration phase was carried out to estimate the values of the isotherm coefficients by minimizing the mean square error (MSE) [78,79] between measured and calculated data. MSE is described by the following equation (7):

$$MSE = \frac{1}{n} \sum_{i=1}^n [y_{cal} - y_{exp}]_i^2 \quad (7)$$

where  $y_{cal}$  is the calculated concentration by the numerical model,  $y_{exp}$  is the measured concentration, and  $n$  is the number of the experimental data point. Values of porosity and bulk density were calculated using the volume of the column part filled with the biochar–sand layer, and the masses and densities of the two materials. In addition, values

of seepage velocity ( $u$ ) were estimated for each test using the solution flow rate, the column section, and the porosity.

The values of the parameters used for the simulation of the two column tests are reported in Table 3.

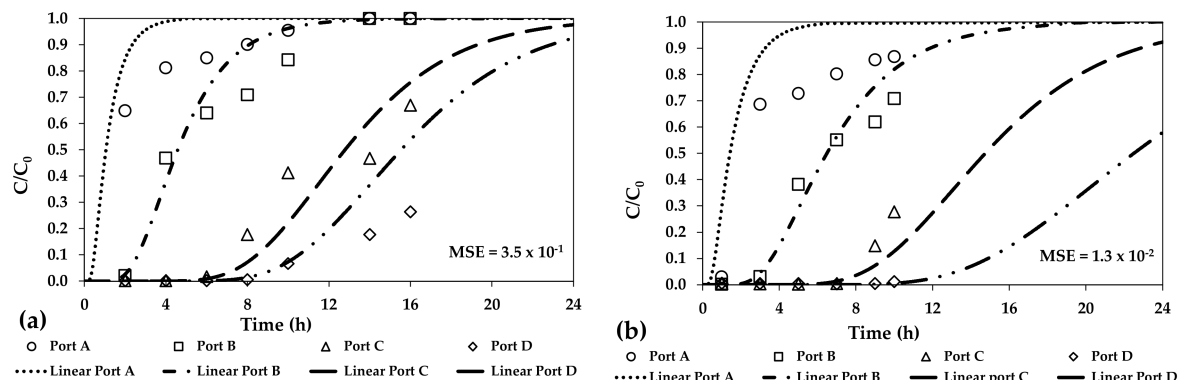


**Figure 3.** Comparison between the experimental data and the numerical ones obtained using linear isotherm for Test 1 (a) and Test 2 (b). The experimental and simulated data were normalized by the respective highest concentration value for both columns.

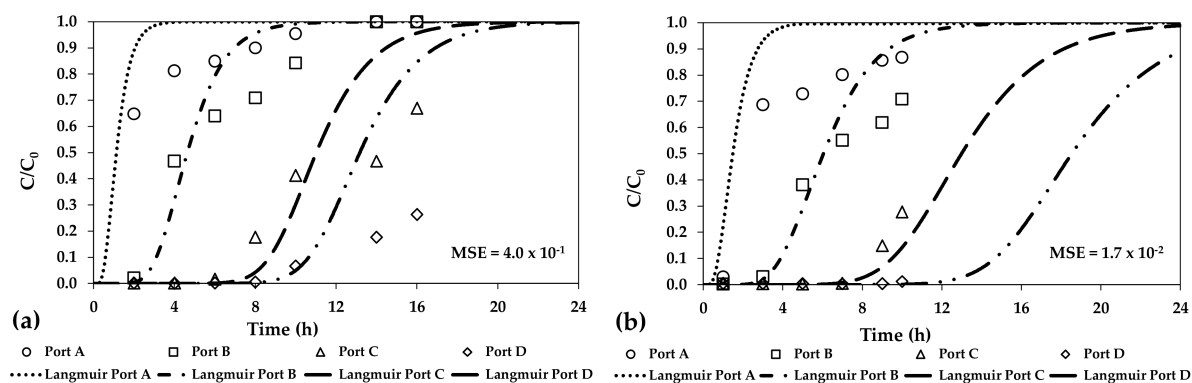


**Figure 4.** Comparison between the experimental data and the numerical ones obtained using Langmuir isotherm for Test 1 (a) and Test 2 (b). The experimental and simulated data were normalized by the respective highest concentration value for both columns.

**Table 3.** Values of the parameters used for the simulation of the two column tests.

Parameter	Unit	Value	
		Test 1	Test 2
$p$	-	0.25	0.30
$D_z$	m	$1.4 \times 10^{-2}$	$1.4 \times 10^{-2}$
$u$	$\text{m min}^{-1}$	$4.0 \times 10^{-3}$	$3.3 \times 10^{-3}$
$D$	$\text{m}^2 \text{min}^{-1}$	$5 \times 10^{-5}$	$5 \times 10^{-5}$
$\rho_b$	$\text{g cm}^{-3}$	1.6	1.6 g
$q_{\max}$	$\text{mg g}^{-1}$	2.6	4.0
$K_L$	$\text{L mg}^{-1}$	$9 \times 10^{-1}$	$9 \times 10^{-1}$
$K_d$	$\text{L mg}^{-1}$	1.6	1.8



The comparison between the MSE values calculated for each test (Figures 3 and 4) demonstrate the similar suitability of both the linear and Langmuir isotherms for simulating the experimental data.

The calibrated values of Langmuir isotherm parameters are comparable to the values reported in the literature for biochars similar in terms of composition to the investigated biochar (Table 4).

**Table 4.** Values of Langmuir isotherm parameters for different types of biochar reported in the literature.

Adsorbent Media	As Conc.	Langmuir Isotherm		References
	(mg L <sup>-1</sup> )	$q_{max}$ (mg/g)	$b$ (L/mg)	
Biochar produced from municipal solid wastes	5–400	18.06–24.49	$7.2 \times 10^{-2}$ – $7.8 \times 10^{-2}$	[80]
Cattle bone char	0.10–1.00	0.399	$1.04 \times 10^{-3}$	[81]
Perilla leaf biochar	0.05–7.00	3.85–7.21	$1.08 \times 10^{-3}$ – $2.14 \times 10^{-3}$	[82]
Peanut shell biochar	5.00	7.94	$2.17 \times 10^{-3}$	[83]
Virgin coniferous wood biochar	1.0	1.8	$9 \times 10^{-2}$	This study

Further numerical tests have been carried out with the aim of testing the sensitivity of the model to a change in the inlet flow (for the residence time effects) and arsenic concentration (for an evaluation of the adsorption effects).

The response of the linear isotherm is predictable, so only the Langmuir isotherm results are reported in the paper. The results show the breakthrough curves of the column (Figure 5).

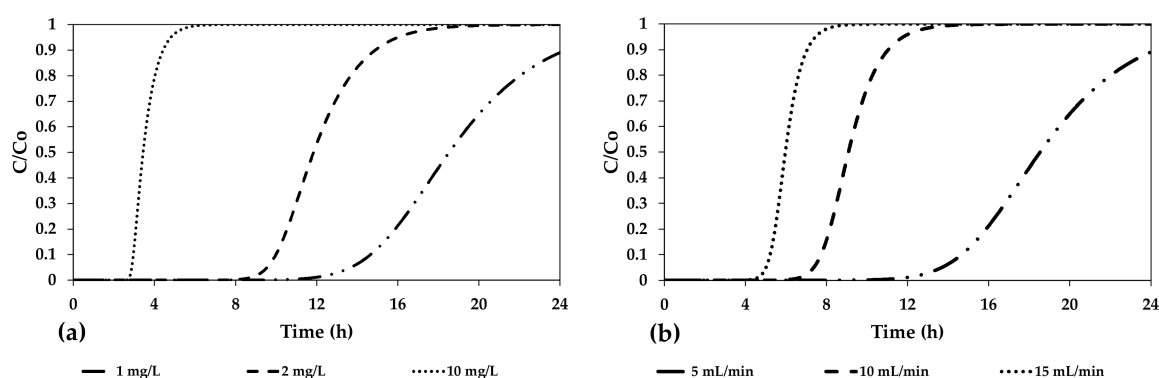


**Figure 5.** The breakthrough curve obtained by numerical simulations increasing the As concentration (a) and the flow of the inflowing solution (b).

It is possible to show, as expected, that when increasing the solute concentration, the capacity of the column diminishes rapidly and the breakthrough of the column is reached more quickly. The same considerations can be derived from the analysis of the data collected with the flow enhancement. The column is not long enough to hold the entire volume of the contaminant.

#### 4. Conclusions

Adsorption of arsenic using a virgin coniferous wood biochar in a fixed bed column was investigated in two ways. Firstly, by preliminary laboratory tests, and secondly by using a numerical model for the calibration of the kinetic parameters and for a short sensitivity analysis.

The column tests measured As removal from contaminated aqueous solutions with a  $C_0$  of 1 mg/L by varying the weight and volume ratio of the biochar in the column system.



The results show that in this case, both the isotherms can be used to describe the behavior of the biochar as an adsorbent of As in dissolved form.

We should note that the extremely small dimension of the material means that the use of large amounts may be unsuitable because zones of low permeability create sub-optimal conditions for contact between the dissolved substance and the active site of the biochar, reducing removal efficiency. It is therefore advisable to conduct lab-scale investigations into the optimal ratio between the filling and adsorbent materials. For this, numerical modeling can contribute to the design aspects.

Virgin coniferous wood biochar is a promising material for use as an adsorbent medium for removing contaminants from groundwater. It is low-cost, and may also contribute to a circular economy due to the fact that it is a waste material.

Starting from these preliminary results, further experiments will be conducted. The results could be useful in implementing the large-scale use of biochar in water treatment or as a remediation technology, i.e., as an adsorbent media of a permeable reactive barrier (PRB), for heavy metal removal from contaminated groundwater.

**Author Contributions:** Conceptualization, M.R.B. and P.V.; methodology, P.V.; software, P.V. and F.T.; validation, M.R., G.M. and A.L.; formal analysis, S.M., G.M. and M.R.; investigation, S.M. and F.T.; resources, M.R.B.; data curation, S.M. and F.T.; writing—original draft preparation, S.M. and F.T.; writing—review and editing, P.V., M.R. and A.L.; visualization, P.V. and F.T.; supervision, M.R.B. and P.V.; project administration, M.R.B.; funding acquisition, M.R.B. All authors have read and agreed to the published version of the manuscript.

**Funding:** This research received no external funding.

**Institutional Review Board Statement:** Not applicable.

**Informed Consent Statement:** Not applicable.

**Data Availability Statement:** The data presented in this study is available on request from the corresponding author.

**Acknowledgments:** The authors wish to thank RECORD IMMOBILIARE S.r.l. who provided RE-CHAR® biochar.

**Conflicts of Interest:** The authors declare no conflict of interest.

## References

1. Mishra, R.K.; Dubey, S.C. Fresh water availability and it's global challenge. *Int. J. Eng. Sci. Invent. Res. Dev.* **2015**, *2*, 351–407.
2. Verma, R.; Dwivedi, P. Heavy metal water pollution-A case study. *Recent Res. Sci. Technol.* **2013**, *5*, 98–99.
3. Egboka, B.C.E.; Nwankwor, G.I.; Orajaka, I.P.; Ejiofor, A.O. Principles and problems of environmental pollution of groundwater resources with case examples from developing countries. *Environ. Health Perspect.* **1989**, *83*, 39–68. [[CrossRef](#)] [[PubMed](#)]
4. Sbarato, V.M.; Sánchez, H.J. Analysis of arsenic pollution in groundwater aquifers by X-ray fluorescence. *Appl. Radiat. Isot.* **2001**, *54*, 737–740. [[CrossRef](#)]
5. Gunduz, O.; Simsek, C.; Hasozbek, A. Arsenic pollution in the groundwater of Simav Plain, Turkey: Its impact on water quality and human health. *Water Air Soil Pollut.* **2010**, *205*, 43–62. [[CrossRef](#)]
6. Liang, C.P.; Wang, S.W.; Kao, Y.H.; Chen, J.S. Health risk assessment of groundwater arsenic pollution in southern Taiwan. *Environ. Geochem. Health* **2016**, *38*, 1271–1281. [[CrossRef](#)] [[PubMed](#)]
7. Habuda-Stanić, M.; Kuleš, M.; Kalajdžić, B.; Romić, Ž. Quality of groundwater in eastern Croatia. The problem of arsenic pollution. *Desalination* **2007**, *210*, 157–162. [[CrossRef](#)]
8. Shah, B.A. Status of groundwater arsenic pollution of Mirzapur district in Holocene aquifers from parts of the Middle Ganga Plain, India. *Environ. Earth Sci.* **2015**, *73*, 1505–1514. [[CrossRef](#)]
9. Zhang, L.; Yang, H.; Tang, J.; Qin, X.; Yu, A.Y. Attenuation of arsenic in a karst subterranean stream and correlation with geochemical factors: A case study at Lihu, South China. *J. Environ. Sci. (China)* **2014**, *26*, 2222–2230. [[CrossRef](#)]
10. Seidl, M.; Balázs, G.; Scheer, M. The Chemistry of Yellow Arsenic. *Chem. Rev.* **2019**, *119*, 8406–8434. [[CrossRef](#)]
11. Zhu, N.; Qiao, J.; Ye, Y.; Yan, T. Synthesis of mesoporous bismuth-impregnated aluminum oxide for arsenic removal: Adsorption mechanism study and application to a lab-scale column. *J. Environ. Manag.* **2018**, *211*, 73–82. [[CrossRef](#)] [[PubMed](#)]
12. Bretzler, A.; Lalanne, F.; Nikiema, J.; Podgorski, J.; Pfenninger, N.; Berg, M.; Schirmer, M. Corrigendum to “Groundwater arsenic contamination in Burkina Faso, West Africa: Predicting and verifying regions at risk” *Sci. Total Environ.* **2017**, *598*, 562. [[CrossRef](#)] [[PubMed](#)]

13. Ratnaike, R.N. Acute and chronic arsenic toxicity. *Postgrad. Med. J.* **2003**, *79*, 391–396. [CrossRef] [PubMed]
14. World Health Organization. *Guidelines for Drinking-Water Quality*, 4th ed.; incorporating the 1st addendum; World Health Organization: Geneva, Switzerland, 2017; ISBN 978-92-4-154995-0. Available online: <https://www.who.int/publications/i/item/9789241549950> (accessed on 26 March 2021).
15. Nicomel, N.R.; Leus, K.; Folens, K.; Van Der Voort, P.; Du Laing, G. Technologies for arsenic removal from water: Current status and future perspectives. *Int. J. Environ. Res. Public Health* **2015**, *13*, 1–24. [CrossRef]
16. Figoli, A.; Fuoco, I.; Apollaro, C.; Chabane, M.; Mancuso, R.; Gabriele, B.; De Rosa, R.; Vespasiano, G.; Barca, D.; Criscuoli, A. Arsenic-contaminated groundwaters remediation by nanofiltration. *Sep. Purif. Technol.* **2020**, *238*, 116461. [CrossRef]
17. Sen, M.; Manna, A.; Pal, P. Removal of arsenic from contaminated groundwater by membrane-integrated hybrid treatment system. *J. Memb. Sci.* **2010**, *354*, 108–113. [CrossRef]
18. Pal, P.; Chakraborty, S.; Linnanen, L. A nanofiltration-coagulation integrated system for separation and stabilization of arsenic from groundwater. *Sci. Total Environ.* **2014**, *476–477*, 601–610. [CrossRef] [PubMed]
19. Košutić, K.; Furač, L.; Sipos, L.; Kunst, B. Removal of arsenic and pesticides from drinking water by nanofiltration membranes. *Sep. Purif. Technol.* **2005**, *42*, 137–144. [CrossRef]
20. Baciocchi, R.; Chiavola, A.; Gavasci, R. Ion exchange equilibria of arsenic in the presence of high sulphate and nitrate concentrations. *Water Sci. Technol. Water Supply* **2005**, *5*, 67–74. [CrossRef]
21. Chiavola, A.; D'Amato, E.; Baciocchi, R. Ion exchange treatment of groundwater contaminated by arsenic in the presence of sulphate. Breakthrough experiments and modeling. *Water. Air. Soil Pollut.* **2012**, *223*, 2373–2386. [CrossRef]
22. Macur, R.E.; Jackson, C.R.; Botero, L.M.; McDermott, T.R.; Inskeep, W.P. Bacterial Populations Associated with the Oxidation and Reduction of Arsenic in an Unsaturated Soil. *Environ. Sci. Technol.* **2004**, *38*, 104–111. [CrossRef]
23. González, M.M.; Gallego, M.; Valcárcel, M. Determination of arsenic in wheat flour by electrothermal atomic absorption spectrometry using a continuous precipitation-dissolution flow system. *Talanta* **2001**, *55*, 135–142. [CrossRef]
24. Ghurye, G.L.; Clifford, D.A.; Tripp, A.R. Combined arsenic and nitrate removal by ion exchange. *J. Am. Water Work. Assoc.* **1999**, *91*, 85–96. [CrossRef]
25. Zhang, H.; Selim, H.M. Kinetics of arsenate adsorption—Desorption in soils. *Environ. Sci. Technol.* **2005**, *39*, 6101–6108. [CrossRef] [PubMed]
26. Boczkaj, G.; Fernandes, A. Wastewater treatment by means of advanced oxidation processes at basic pH conditions: A review. *Chem. Eng. J.* **2017**, *320*, 608–633. [CrossRef]
27. Boni, M.R.; Chiavola, A.; Di Marcantonio, C.; Sbaffoni, S.; Biagioli, S.; Cecchini, G.; Frugis, A. A study through batch tests on the analytical determination and the fate and removal of methamphetamine in the biological treatment of domestic wastewater. *Environ. Sci. Pollut. Res.* **2018**, *25*, 27756–27767. [CrossRef]
28. Chiavola, A.; Tedesco, P.; Boni, M.R. Fate of selected drugs in the wastewater treatment plants (WWTPs) for domestic sewage. *Environ. Sci. Pollut. Res.* **2019**, *26*, 1113–1123. [CrossRef] [PubMed]
29. Karimi, S.; Tavakkoli Yarak, M.; Karri, R.R. A comprehensive review of the adsorption mechanisms and factors influencing the adsorption process from the perspective of bioethanol dehydration. *Renew. Sustain. Energy Rev.* **2019**, *107*, 535–553. [CrossRef]
30. Chiavola, A.; Tedesco, P.; Boni, M.R. Fate of Some Endocrine Disruptors in Batch Experiments Using Activated and Inactivated Sludge. *Water Air Soil Pollut.* **2016**, *227*, 424. [CrossRef]
31. Thirunavukkarasu, V.; Anuradha, C.V.; Viswanathan, P. Protective effect of fenugreek (*Trigonella foenum graecum*) seeds in experimental ethanol toxicity. *Phyther. Res.* **2003**, *17*, 737–743. [CrossRef]
32. Pattanayak, J.; Mondal, K.; Mathew, S.; Lalvani, S.B. A Parametric evaluation of the removal of As(V) and As(III) by carbon-based adsorbents. *Carbon N.Y.* **2000**, *38*, 589–596. [CrossRef]
33. Guha, S.; Chaudhury, P. Locating critical points and constructing reaction paths in noble gas clusters: A simulated annealing based study. *J. Mol. Struct. THEOCHEM* **2010**, *945*, 12–16. [CrossRef]
34. Tchieda, V.K.; D'Amato, E.; Chiavola, A.; Parisi, M.; Chianese, A.; Amamra, M.; Kanaev, A. Removal of Arsenic by Alumina: Effects of Material Size, Additives, and Water Contaminants. *Clean Soil Air Water* **2016**, *44*, 496–505. [CrossRef]
35. Chiavola, A.; D'Amato, E.; Boni, M.R. Comparison of different iron oxide adsorbents for combined arsenic, vanadium and fluoride removal from drinking water. *Int. J. Environ. Sci. Technol.* **2019**, *16*, 6053–6064. [CrossRef]
36. Chiavola, A.; D'Amato, E.; Stoller, M.; Chianese, A.; Boni, M.R. Application of iron based nanoparticles as adsorbents for Arsenic removal from water. *Chem. Eng. Trans.* **2016**, *47*, 325–330. [CrossRef]
37. Sawana, R.; Somasundar, Y.; Iyer, V.S.; Baruwati, B. Ceria modified activated carbon: An efficient arsenic removal adsorbent for drinking water purification. *Appl. Water Sci.* **2017**, *7*, 1223–1230. [CrossRef]
38. Kalaruban, M.; Loganathan, P.; Nguyen, T.V.; Nur, T.; Hasan Johir, M.A.; Nguyen, T.H.; Trinh, M.V.; Vigneswaran, S. Iron-impregnated granular activated carbon for arsenic removal: Application to practical column filters. *J. Environ. Manag.* **2019**, *239*, 235–243. [CrossRef] [PubMed]
39. Vithanage, M.; Herath, I.; Joseph, S.; Bundschuh, J.; Bolan, N.; Ok, Y.S.; Kirkham, M.B.; Rinklebe, J. Interaction of arsenic with biochar in soil and water: A critical review. *Carbon N.Y.* **2017**, *113*, 219–230. [CrossRef]
40. Igalavithana, A.D.; Kwon, E.E.; Vithanage, M.; Rinklebe, J.; Moon, D.H.; Meers, E.; Tsang, D.C.W.; Ok, Y.S. Soil lead immobilization by biochars in short-term laboratory incubation studies. *Environ. Int.* **2019**, *127*, 190–198. [CrossRef]

41. Zimmerman, A.R.; Gao, B.; Ahn, M.Y. Positive and negative carbon mineralization priming effects among a variety of biochar-amended soils. *Soil Biol. Biochem.* **2011**, *43*, 1169–1179. [\[CrossRef\]](#)
42. Viotti, P.; Tatti, F.; Rossi, A.; Luciano, A.; Marzeddu, S.; Mancini, G.; Boni, M.R. An Eco-Balanced and Integrated Approach for a More-Sustainable MSW Management. *Waste Biomass Valorization* **2020**, *11*, 5139–5150. [\[CrossRef\]](#)
43. Stoller, M.; Sacco, O.; Vilardi, G.; Pulido, J.M.O.; Di Palma, L. Technical–economic evaluation of chromium recovery from tannery wastewater streams by means of membrane processes. *Desalin. Water Treat.* **2018**, *127*, 57–63. [\[CrossRef\]](#)
44. Agegnehu, G.; Srivastava, A.K.; Bird, M.I. The role of biochar and biochar-compost in improving soil quality and crop performance: A review. *Appl. Soil Ecol.* **2017**, *119*, 156–170. [\[CrossRef\]](#)
45. Glazunova, D.M.; Kuryntseva, P.A.; Selivanovskaya, S.Y.; Galitskaya, P.Y. Assessing the Potential of Using Biochar as a Soil Conditioner. In *IOP Conference Series: Earth and Environmental Science, Proceedings of the 3rd International Conference Environment and Sustainable Development of Territories: Ecological Challenges of the 21st Century, Kazan, Russia, 27–29 September 2017*; Institute of Physics Publishing: Bristol, UK, 2018; Volume 107, p. 12059.
46. Ding, Y.; Liu, Y.; Liu, S.; Li, Z.; Tan, X.; Huang, X.; Zeng, G.; Zhou, L.; Zheng, B. Biochar to improve soil fertility. A review. *Agron. Sustain. Dev.* **2016**, *36*, 1–18. [\[CrossRef\]](#)
47. Fidel, R.; Laird, D.; Parkin, T. Effect of Biochar on Soil Greenhouse Gas Emissions at the Laboratory and Field Scales. *Soil Syst.* **2019**, *3*, 8. [\[CrossRef\]](#)
48. Criscuoli, I.; Ventura, M.; Sperotto, A.; Panzacchi, P.; Tonon, G. Effect of woodchips biochar on sensitivity to temperature of soil greenhouse gases emissions. *Forests* **2019**, *10*, 594. [\[CrossRef\]](#)
49. Keske, C.; Godfrey, T.; Hoag, D.L.K.; Abedin, J. Economic feasibility of biochar and agriculture coproduction from Canadian black spruce forest. *Food Energy Secur.* **2020**, *9*, e188. [\[CrossRef\]](#)
50. Ahmed, M.B.; Zhou, J.L.; Ngo, H.H.; Guo, W. Insight into biochar properties and its cost analysis. *Biomass Bioenergy* **2016**, *84*, 76–86. [\[CrossRef\]](#)
51. Yao, Z.; You, S.; Ge, T.; Wang, C.H. Biomass gasification for syngas and biochar co-production: Energy application and economic evaluation. *Appl. Energy* **2018**, *209*, 43–55. [\[CrossRef\]](#)
52. Ng, W.C.; You, S.; Ling, R.; Gin, K.Y.H.; Dai, Y.; Wang, C.H. Co-gasification of woody biomass and chicken manure: Syngas production, biochar reutilization, and cost-benefit analysis. *Energy* **2017**, *139*, 732–742. [\[CrossRef\]](#)
53. Viglašová, E.; Galamboš, M.; Danková, Z.; Krivosudský, L.; Lengauer, C.L.; Hood-Nowotny, R.; Soja, G.; Rempel, A.; Matík, M.; Briančin, J. Production, characterization and adsorption studies of bamboo-based biochar/montmorillonite composite for nitrate removal. *Waste Manag.* **2018**, *79*, 385–394. [\[CrossRef\]](#) [\[PubMed\]](#)
54. Frišták, V.; Micháleková-Richveisová, B.; Viglašová, E.; Ďuriška, L.; Galamboš, M.; Moreno-Jiménez, E.; Pipiška, M.; Soja, G. Sorption separation of Eu and As from single-component systems by Fe-modified biochar: Kinetic and equilibrium study. *J. Iran. Chem. Soc.* **2017**, *14*, 521–530. [\[CrossRef\]](#)
55. Daňo, M.; Viglašová, E.; Galamboš, M.; Štamberg, K.; Kujan, J. Surface Complexation Models of Pertechetate on Biochar/Montmorillonite Composite—Batch and Dynamic Sorption Study. *Materials* **2020**, *13*, 3108. [\[CrossRef\]](#) [\[PubMed\]](#)
56. Sizmur, T.; Quilliam, R.; Puga, A.P.; Moreno-Jiménez, E.; Beesley, L.; Gomez-Eyles, J.L. Application of Biochar for Soil Remediation. *98104* **2015**, 295–324. [\[CrossRef\]](#)
57. Hu, X.; Ding, Z.; Zimmerman, A.R.; Wang, S.; Gao, B. Batch and column sorption of arsenic onto iron-impregnated biochar synthesized through hydrolysis. *Water Res.* **2015**, *68*, 206–216. [\[CrossRef\]](#)
58. Qambrani, N.A.; Rahman, M.M.; Won, S.; Shim, S.; Ra, C. Biochar properties and eco-friendly applications for climate change mitigation, waste management, and wastewater treatment: A review. *Renew. Sustain. Energy Rev.* **2017**, *79*, 255–273. [\[CrossRef\]](#)
59. Boni, M.R.; Chiavola, A.; Marzeddu, S. Remediation of Lead-Contaminated Water by Virgin Coniferous Wood Biochar Adsorbent: Batch and Column Application. *Water Air Soil Pollut.* **2020**, *231*, 171. [\[CrossRef\]](#)
60. Tatti, F.; Papini, M.P.; Sappa, G.; Raboni, M.; Arjmand, F.; Viotti, P. Contaminant back-diffusion from low-permeability layers as affected by groundwater velocity: A laboratory investigation by box model and image analysis. *Sci. Total Environ.* **2018**, *622–623*, 164–171. [\[CrossRef\]](#) [\[PubMed\]](#)
61. Tatti, F.; Petrangeli Papini, M.; Torretta, V.; Mancini, G.; Boni, M.R.; Viotti, P. Experimental and numerical evaluation of Groundwater Circulation Wells as a remediation technology for persistent, low permeability contaminant source zones. *J. Contam. Hydrol.* **2019**, *222*, 89–100. [\[CrossRef\]](#)
62. Grund, S.C.; Hanusch, K.; Wolf, H.U. Arsenic and Arsenic Compounds. In *Ullmann's Encyclopedia of Industrial Chemistry*; Wiley-VCH Verlag GmbH & Co. KGaA: Weinheim, Germany, 2008; Volume 100 C, pp. 41–93.
63. Boni, M.R.; Leoni, S.; Sbaffoni, S. Co-landfilling of pretreated waste: Disposal and management strategies at lab-scale. *J. Hazard. Mater.* **2007**, *147*, 37–47. [\[CrossRef\]](#)
64. Chiavola, A.; Marzeddu, S.; Boni, M.R. Remediation of Water Contaminated by Pb(II) Using Virgin Coniferous Wood Biochar as Adsorbent. In *Frontiers in Water-Energy-Nexus—Nature-Based Solutions, Advanced Technologies and Best Practices for Environmental Sustainability. Advances in Science, Technology & Innovation (IEREK Interdisciplinary Series for Sustainable Development); Proceedings of the 2nd WaterEnergyNEXUS Conference*; Salerno, Italy, 14–17 November 2018; Naddeo, V., Balakrishnan, M., Choo, K.-H., Eds.; Springer, Cham: Salerno, Italy, 2020; pp. 363–366; ISBN 978-3-030-13067-1. [\[CrossRef\]](#)
65. Rose, P.; Hager, S.; Glas, K.; Rehmann, D.; Hofmann, T. Coating techniques for glass beads as filter media for removal of manganese from water. *Water Sci. Technol. Water Supply* **2017**, *17*, 95–106. [\[CrossRef\]](#)

66. Boni, M.R.; Chiavola, A.; Antonucci, A.; Di Mattia, E.; Marzeddu, S. A novel treatment for Cd-contaminated solution through adsorption on beech charcoal: The effect of bioactivation. *Desalin. Water Treat.* **2018**, *127*, 104–110. [[CrossRef](#)]
67. Boni, M.R.; Chiavola, A.; Marzeddu, S. Application of Biochar to the Remediation of Pb-Contaminated Solutions. *Sustainability* **2018**, *10*, 4440. [[CrossRef](#)]
68. *Metodi analitici per le acque*; Belli, M.; Centioli, D.; De Zorzi, P.; Sansone, U.; Capri, S.; Pagnotta, R.; Pettine, M. (Eds.) APAT—IRSA/CNR: Rome, Italy, 2003; ISBN 88-448-0083-7.
69. Clesceri, L.S.; Greenberg, A.E.; Eaton, A.D. (Eds.) *Standard Methods for the Examination of Water and Wastewater*, 20th ed.; American Public Health Association (APHA): Washington, DC, USA, 1998; ISBN 978-0875532356.
70. Pickens, J.F.; Grisak, G.E. Scale-dependent dispersion in a stratified granular aquifer. *Water Resour. Res.* **1981**, *17*, 1191–1211. [[CrossRef](#)]
71. Luciano, A.; Viotti, P.; Torretta, V.; Mancini, G. Numerical approach to modelling pulse-mode soil flushing on a Pb-contaminated soil. *J. Soils Sediments* **2013**, *13*, 43–55. [[CrossRef](#)]
72. Vilardi, G.; Mpouras, T.; Dermatas, D.; Verdone, N.; Polydera, A.; Di Palma, L. Nanomaterials application for heavy metals recovery from polluted water: The combination of nano zero-valent iron and carbon nanotubes. Competitive adsorption non-linear modeling. *Chemosphere* **2018**, *201*, 716–729. [[CrossRef](#)] [[PubMed](#)]
73. Langmuir, I. The adsorption of gases on plane surfaces of glass, mica and platinum. *J. Am. Chem. Soc.* **1918**, *40*, 1361–1403. [[CrossRef](#)]
74. Karahan, H. Unconditional stable explicit finite difference technique for the advection-diffusion equation using spreadsheets. *Adv. Eng. Softw.* **2007**, *38*, 80–86. [[CrossRef](#)]
75. Saul'yev, V.K. *Integration of Equations of Parabolic Type by the Method of Nets*; Pergamon Press Ltd.: Oxford, UK, 1964; ISBN 978-0-08-010195-8.
76. Bhattacharya, P.; Welch, A.H.; Stollenwerk, K.G.; McLaughlin, M.J.; Bundschuh, J.; Panaullah, G. Arsenic in the environment: Biology and Chemistry. *Sci. Total Environ.* **2007**, *379*, 109–120. [[CrossRef](#)]
77. Cullen, W.R.; Reimer, K.J. Arsenic speciation in the environment. *Chem. Rev.* **1989**, *89*, 713–764. [[CrossRef](#)]
78. Tan, K.L.; Hameed, B.H. Insight into the adsorption kinetics models for the removal of contaminants from aqueous solutions. *J. Taiwan Inst. Chem. Eng.* **2017**, *74*, 25–48. [[CrossRef](#)]
79. Vilardi, G.; Di Palma, L.; Verdone, N. Heavy metals adsorption by banana peels micro-powder: Equilibrium modeling by non-linear models. *Chinese, J. Chem. Eng.* **2018**, *26*, 455–464. [[CrossRef](#)]
80. Jin, H.; Capareda, S.; Chang, Z.; Gao, J.; Xu, Y.; Zhang, J. Biochar pyrolytically produced from municipal solid wastes for aqueous As(V) removal: Adsorption property and its improvement with KOH activation. *Bioresour. Technol.* **2014**, *169*, 622–629. [[CrossRef](#)] [[PubMed](#)]
81. Begum, S.A.; Golam Hyder, A.H.M.; Vahdat, N. Adsorption isotherm and kinetic studies of As(V) removal from aqueous solution using cattle bone char. *J. Water Supply Res. Technol.—AQUA* **2016**, *65*, 244–252. [[CrossRef](#)]
82. Niazi, N.K.; Bibi, I.; Shahid, M.; Ok, Y.S.; Burton, E.D.; Wang, H.; Shaheen, S.M.; Rinklebe, J.; Lüttge, A. Arsenic removal by perilla leaf biochar in aqueous solutions and groundwater: An integrated spectroscopic and microscopic examination. *Environ. Pollut.* **2018**, *232*, 31–41. [[CrossRef](#)] [[PubMed](#)]
83. Sattar, M.S.; Shakoor, M.B.; Ali, S.; Rizwan, M.; Niazi, N.K.; Jilani, A. Comparative efficiency of peanut shell and peanut shell biochar for removal of arsenic from water. *Environ. Sci. Pollut. Res.* **2019**, *26*, 18624–18635. [[CrossRef](#)] [[PubMed](#)]